General Disclaimer

One or more of the Following Statements may affect this Document

- This document has been reproduced from the best copy furnished by the organizational source. It is being released in the interest of making available as much information as possible.

- This document may contain data, which exceeds the sheet parameters. It was furnished in this condition by the organizational source and is the best copy available.

- This document may contain tone-on-tone or color graphs, charts and/or pictures, which have been reproduced in black and white.

- This document is paginated as submitted by the original source.

- Portions of this document are not fully legible due to the historical nature of some of the material. However, it is the best reproduction available from the original submission.

NASA TECHNICAL MEMORANDUM

NASA TM X-71820

NASA TM X-71820

GEOMETRY EFFECTS ON STOL ENGINE-OVER-THE-WING ACOUSTICS WITH 5:1 SLOT NOZZLES

by U. von Glahn and D. Groesbeck
Lewis Research Center
Cleveland, Ohio 44135

TECHNICAL PAPER to be presented at
Ninetieth Meeting of the Acoustical
Society of America
San Francisco, California, November 4-7, 1975

GEOMETRY EFFECTS ON STOL ENGINE-OVER-THE-WING ACOUSTICS WITH 5:1 SLOT NOZZLES

by U. von Glahn and D. Groesbeck

National Aeronautics and Space Administration
Lewis Research Center
Cleveland, Ohio 44135

E-8519

ABSTRACT

The correspondence of far field acoustic trends with changes in the characteristics of the flow field at the wing trailing edge caused by alterations in the nozzle-wing geometry were determined at model scale with a 5:1 slot nozzle (equivalent diameter, 5.1 cm) for several STOL-OTW configurations. Nozzle roof angles of 10° to 40° were tested with and without cutback of the nozzle sidewalls. Also included, for comparison, was a 5:1 slot nozzle with various external deflectors. Three wing chord sizes were used: baseline (33 cm with flaps retracted), 2/3-baseline and 3/2-baseline. Flap deflection angles of 20° and 60° were used. The nozzle locations were at 21 and 46-percent of chord. With increasing wing size, representing several airframe/engine installations, the jet noise shielding benefits increased. With increasing nozzle roof angle, the jet velocity at the trailing edge was decreased, causing a decrease in trailing-edge and fluctuating lift noise. Cutback of the nozzle sides improved flow attachment and reduced far-field noise. The best flow attachment and least trailing-edge noise generally were obtained with a 40° external deflector configuration and a cutback nozzle with a 40° roof angle.

INTRODUCTION

In order to help meet acceptable community noise standards for future short takeoff and landing (STOL) aircraft, the engine exhaust nozzle can be placed over the wing (OTW). The shielding of jet-noise radiated to the ground accomplished by such an engine-wing configuration is similar to that observed on the ground by the erection of a barrier between a noise source and an observer.

With a STOL-OTW configuration, the most prominent noise sources, as indicated in figure 1 appear to be the engine exhaust jet noise, engine core noise, external deflector (if used), scrubbing or fluctuating lift noise produced by the exhaust flow over the wing surface, and wing trailing edge noise caused by an interaction between the edge and the jet flow.

The noise shielding capability of a wing for the STOL engine-over-the-wing concept has been studied experimentally with several small-scale models (refs. 1 to 4) and to a more limited extent with a large-scale configuration (ref. 5). A typical STOL OTW configuration noise spectrum is shown in figure 2. Currently it is believed, though not completely substantiated by theory and experiment, that the noise in the low frequency region is caused by the fluctuating lift noise source (noise source I), while that in the mid-frequency range is caused by trailing edge noise (noise source II). In the high frequency range, the shielding surface attenuates the jet noise by the principle of barrier shielding; the amount of shielding depends on a variety of factors including surface length, nozzle configuration, and nozzle size (refs. 1-4).

The purpose of the present study, conducted at the NASA Lewis Research Center, was to establish the acoustic trends corresponding to changes in the flow field characteristics at the wing trailing edge caused by variations in nozzle geometry, chordwise location of the nozzles, wing chord size, and flap deflection angle. The work is an extension of the flat plate study of reference 6 to curved shielding surfaces representing possible STOL-OTW configurations. Data were obtained with 5:1 aspect ratio slot nozzles (effective diameter, 5.1 cm) in which the nozzle roof angle (kick-down angle) was varied from 10° to 40°, the nozzle sides were cut-back from 0° to 40°, and, finally, a simple 5:1 slot nozzle with several deflectors.

The baseline shielding surfaces (wings) corresponded in size and shape to the airfoil and flap deflections of 20° and 60° (corresponding to takeoff and landing settings, respectively) used in references 1 and 2. In addition, shielding surfaces of 2/3- and 1½-times the size of the baseline wings were also used. The baseline nozzle-wing configurations are representative of a twin-engine OTW aircraft application. The 2/3-size nozzle-wing configurations are representative of a siamese-twin engine nacelle OTW aircraft application. Finally, the 1½-size nozzle-wing configurations are representative of a 4-engine, separate nacelle OTW aircraft configuration. The span of all wings was 61 cm.

Mach number contour maps at the wing trailing edge were obtained for all configurations. From these, the jet flow Mach number profiles at the wing trailing edges in the plane of the nozzle centerline and normal to the wing were obtained. Acoustic data were taken only at 90° to the normal chordline of the airfoils with flaps retracted. A nominal jet velocity of 266 m/sec was used to obtain aerodynamic and acoustic data for all test configurations. Acoustic data were also obtained at 200 m/sec.

APPARATUS AND PROCEDURE

Facility

The noise tests were conducted using an out-of-doors facility within the 7x15 m courtyard of a subsonic wind tunnel at the Lewis Research Center.

This facility is described in detail in reference 6. Open-cell foam pads were used in an effort to minimize reflections from the surrounding walls. In addition, foam pads were also placed on the ground to minimize ground reflection effects on the acoustic data.

Sound pressure level (SPL) spectra were obtained using a 1.27-cm diameter condenser microphone with wind screen. Data were recorded at 90° to the jet axis at a micropnone distance of 3.05 meters. The noise data were recorded on a FM tape recorder and digitized by a four second time averaged one-third octave band spectrum analyzer. The analyzer determined sound pressure level spectra in decibels referenced to 2×10^{-5} N/m^2.

Jet Mach number (velocity) profiles were obtained at the trailing edge of the shielding surfaces. Measurements were made with a traversing pitot tube with an entrance cone angle of 60° to help minimize flow angularity effects resulting from the jet flow over the curved surfaces. A vane on the traversing equipment was used to establish the jet flow angle for each traverse. When the flow angle, as determined by means of the vane, exceeded the angularity capability of the pitot tube, the tube angle to the local flow was adjusted to provide suitable data. The pressures measured were transmitted to an x-y-y' plotter which yielded direct traces on graph paper of the total pressure distribution across the jet.

Acoustic data were taken at nominal jet velocities of 200 and 266 m/sec while aerodynamic data were taken at a nominal jet velocity of 266 m/sec.

Models

The test nozzles consisted of the 5:1 slot nozzles shown in figure 3. The nozzles all had equivalent diameters of 5.1 cm. A single straight-sided nozzle was used for the tests without nozzle sidewall cutback. The roof angle for this nozzle was changed by providing inserts that altered the angle from 10° to 40° in 10° increments. Separate nozzles were provided for the cases with sidewall cutback. The cutback angle was the same as the roof angle for each respective nozzle. The sidewalls of all these nozzles were parallel.

A simple 5:1 slot nozzle (ref. 6) was used with various deflectors (fig. 3(g)). Each of the sides of the nozzle converged at 5° and the nominal nozzle dimensions at the exhaust plane was 2.0 cm by 10.2cm. The 40° full-lip deflector was similar to that used in reference 4.

The shielding surfaces are shown schematically in figure 4 together with pertinent dimensions. The surfaces consisted of metal plates secured to wooden ribs. The surfaces approximated the upper surface contours of the airfoils with 20° and 60° deflected flaps used in references 1 and 2.

All wings had a span of 61 cm. As indicated in figure 4, the nozzles were located at two axial locations on the surfaces corresponding to nominal airfoil chordwise stations of 21- and 46-percent with flaps retracted.

The nozzles are referred to by their roof and cutback angles; for example, the nozzle with a 20° roof angle and 20° sidewall cutback angle is designated by "20/20" while the nozzle with a roof angle of 20° and no sidewall cutback is designated by "20/0". The wings will be referred to by the flap deflection angle, 20° or 60°, and their relative size given by 2/3-baseline, baseline and 3/2-baseline. The equivalent flaps-retracted chord sizes for these wings are 22, 33, and 49.5 cm respectively.

A photograph of a representative nozzle-wing configuration installed in the test rig for flow field measurements is shown in figure 5.

AERODYNAMIC DATA

Representative velocity contour maps illustrating the flow field changes at the wing trailing edge location caused by alterations in geometry are shown in figures 6 to 16. The velocity data are shown in terms of constant local Mach number lines in a spanwise plane normal to the wing surface at the wing trailing edge. Velocity profiles (in terms of local Mach number) in this plane were determined at the nozzle centerline in a direction perpendicular to the wing surface. The correspondence of the trends in the profile shapes and absolute velocities with nozzle-wing geometry changes, as will be shown later, are then compared with the measured acoustic characteristics for these configurations.

Effect of nozzle roof angle. - The effect of increasing the nozzle roof angle was to decrease the thickness of the jet shear layer at the wing trailing edge and, at the same time, decrease the peak local Mach number (figs. 6 and 7). The flow changes were accompanied by greater spanwise spreading of the jet flow for constant local Mach number contour lines.

Effect of nozzle sidewall cutback. - For constant nozzle roof angles, the effect of nozzle sidewall cutback was to reduce the thickness of the jet shear layer and decrease the peak local Mach number (fig. 8). At the same time, cutback of the nozzle sidewalls also increased the spanwise spreading of the jet flow at the wing trailing edge.

Effect of nozzle chordwise location. - The effect of locating the nozzles closer to the trailing edges of the wings (0.46 chord) was to decrease the thickness of the jet shear layer and increase the peak local Mach number (compare fig. 9 with fig. 6 and see also fig. 10). The flow contours at the 0.46 chord location for nozzles with roof angles of 10° and 20° indicated some tendency for the flow to separate off the wing surface at the trailing edge (fig. 9(a) and 9(b)).

Effect of wing size. - The effect of wing size on the aerodynamic characteristics is shown in figures 11 to 13. With increasing wing size, the spanwise spread of the jet flow is decreased while the jet shear layer thickness is increased. At the same time, the peak local Mach number at the wing trailing edge decreases with increasing wing size.

Effect of external deflector variations. - The flow field contours for the two 40° deflectors used with the simple 5:1 slot nozzle are shown in figures 14 and 15. In general, the effect of a change in chordwise location of the nozzle on the flow field at the wing trailing edge were similar to those discussed previously. A reduction in the deflector lip size (full-lip to 1/2-lip, see fig. 3) caused both the jet shear layer thickness and peak local Mach number to increase. A reduction in the deflector angle, θ, from 40° to 30° for the full-lip deflector (not shown) caused small increases in the jet shear layer thickness and peak local Mach number.

Comparison of flow fields with and without external deflector. - A comparison of the flow fields obtained at the wing trailing edge with the 40/40 nozzle and those obtained with the simple 5:1 slot nozzle using the 40° full-lip deflector is shown in figure 16. It is apparent that the flow fields with the external deflector configuration have a much thinner jet shear layer and lower peak local Mach numbers than those with the cutback nozzle.

CORRESPONDENCE OF OTW AERO-ACOUSTIC DATA

Representative aerodynamic trends caused by changes in nozzle-wing geometry and their corresponding effects on acoustic characteristics are shown by the data in figures 17 and 24. The aerodynamic data are presented in terms local Mach number at the wing trailing edge as a function of distance above the surface (normal to the chord) at nozzle centerline. The acoustic data are presented in terms of sound pressure level spectra. In addition to the nozzle-wing spectra, the nozzle-only spectrum for the simple 5:1 slot nozzle is also shown as a reference level.

The 5:1 slot nozzle was selected as a reference level for all the nozzle-wing configurations because the wing surface initially turns the flow from the nozzles effectively parallel to the surface regardless of the nozzle roof angle. However, the nozzle roof angle does influence the spanwise spread of the jet exhaust and consequently helps determine the thickness of the jet shear layer and the local jet velocity at the wing trailing edge. In order to obtain a reference nozzle-only spectrum free of these flow turning and spreading effects, the spectrum of the simple 5:1 slot nozzle was chosen. Each set of aerodynamic and acoustic data are presented on the same figure to permit a convenient means for appraising the correspondence between the aerodynamic and acoustic data trends. Except as noted the data shown are for a jet velocity of 266 m/sec.

Nozzle-Wing Configurations Without External Deflector

The correspondence of nozzle-wing geometry changes on the flow field at the wing trailing edge and the far field noise are summarized in the following sections for nozzles without an external deflector. While most of the discussion centers about the baseline wing, trends similar to those discussed were observed with all nozzle-wing configurations.

Roof (kickdown) angle. - The effect of roof angle on the aero-acoustic characteristics of the baseline wing configurations are shown in figure 17 for the nozzles with sidewall cutback. With increasing roof angle, the jet shear layer at the trailing edge decreases in thickness. In addition, the peak local Mach number is also reduced. The reductions in jet shear layer thickness and peak velocity with increasing nozzle roof angle results in an overall reduction in the sound pressure levels in the frequency ranges in which the nozzle-wing noise level is greater than that of the nozzle only. In the high frequency region, where jet noise shielding by the wing can occur, the noise level was generally slightly reduced with increasing nozzle roof angle (1-3 dB, depending on the configuration).

For the nozzles without nozzle sidewall cutback, increasing the roof angle did not reduce the low frequency noise as much as for those with nozzle sidewall cutback (fig. 18). At high frequencies, the reduction in noise level (shielding benefits) with increasing nozzle roof angle noted for the cutback nozzles generally was not observed for the nozzles without sidewall cutback. In all cases, nozzles with roof angles of 10° and 20° did not provide good flow attachment for the 60° flap deflection wing configurations. Consequently, these nozzles generally were eliminated from this portion of the acoustic study.

All cutback nozzle-wing configurations tested, except the baseline wing configuration with 60° flap deflection, showed the location of noise source I (see fig. 2) to be in the range of 315 to 500 hertz. With a 60° flap deflection, noise source I for the baseline nozzle-wing configuration occurred at 250 hertz. No reason can be given at this time for this anomaly. In general, noise source II (see fig. 2) occurred in the frequency range between 1000 and 2000 hertz. Noise source I was substantially independent of jet velocity and wing size. Noise source II varied directly with wing size. No effect of roof or cutback angles on the location of the peak frequency for noise sources I and II was noted.

A comparison of the spectra for the baseline wing configuration (40/40 nozzle) with jet exhaust velocities of 200 and 266 m/sec is shown in figure 19. It is apparent that the change in noise level due to the difference in jet velocities is greater for noise source II (~9 dB) than that for noise source I (~4 dB). A preliminary analysis of all the data taken indicates that, with a constant jet velocity, the reduction in noise level with increasing roof angle appears generally to follow a 3-power law of the peak local velocity at the trailing edge for noise source I (peak SPL in 250 to 500 Hz range). Noise source II (peak SPL in 1000 to 2000 Hz range) appears

generally to follow a 6-power law of the peak local velocity at the trailing edge.

Chordwise location of nozzle. - Positioning of the nozzle closer to the trailing edge (0.46 chord) generally caused the thickness of the jet shear layer at the trailing edge to decrease compared to that at the baseline location (0.21 chord). At the same time, however, the peak local velocity at the trailing edge was increased by as much as 25-percent. Representative examples of this trend are shown in figure 20 for the cutback nozzles. In general, the noise level of source I (see fig. 2) decreased only slightly between the two chordwise locations. However, at the higher frequencies, associated with noise source II, the noise level increased significantly with the nozzle located closer to the trailing edge. This increase in noise level is caused, in part, by the shorter chord length available for shielding the jet noise. Indeed, with the nozzle placed at 0.46 chord for the 20° flap configuration (fig. 9), no jet noise shielding was obtained up to 20 kHz. As was noted previously for this nozzle chordwise location, the flow contours at the trailing edge with a 20° flap deflection and a 10° roof angle showed evidence of flow separation at the spanwise boundaries of the jet flow. However, the acoustic data showed no significant effect of this flow separation on the noise level.

Wing size. - For a given nozzle located at a fixed chordwise location, an increase in wing size caused the jet shear layer thickness to increase while the peak local Mach number decreased (fig. 21). In addition, the location (height) of the peak local velocity from the surface at the wing trailing edge tended to increase with increasing chord size; significantly so for the largest wing with a 60° flap deflection indicating some flow separation from the surface. With a 20° flap deflection (fig. 21(a)), the noise level is markedly reduced with increasing wing size at frequencies greater than 315 Hz. With a 60° flap deflection (fig. 21(b)), the noise levels above 500 Hz also are reduced with increasing wing size; however, the noise level at low frequencies (noise source I) is only slightly reduced for the configurations shown. A gross comparison of the 20° and 60° flap configurations of figure 21, indicates similar noise levels for the respective wing sizes except in the region of noise source I, where the 20° flap configuration for the largest wing is quieter (~3 dB) than the 60° flap configuration. Comparison of the velocity profiles at the trailing edges for the various wing sizes indicates that the 60° flap velocity profiles are much thicker and the peak local Mach numbers are less (up to 20-percent for the largest wing) than those for the 20° flap. The trends shown in figure 21 are typical of those for the other nozzle and wing combinations tested.

Nozzle-Wing Configurations With External Deflector

The aerodynamic characteristics of the 40° external deflector (full- and half-lip configurations) are shown in figures 22 and 23 together with the corresponding acoustic spectra.

Deflector lip size. - A reduction in lip size from full to one-half (see fig. 3) caused both the jet shear layer thickness at the trailing edge and the peak local jet Mach number to increase (fig. 22). As a consequence, the smaller deflector lip size produced an increase in the noise level over that for the full-sized deflector lip in the mid and high frequency range by as much as 3 dB. No significant effect of deflector lip size on noise level was noted for noise source I (low frequencies). As was the case for the baseline nozzle-wing configurations with an external deflector, the peak noise level for noise source II occurred near 1250 Hz with both the 20° and 60° flaps, however, the frequency for the peak noise level of source I was at 400 Hz for the 20° flap and 250 Hz for the 60° flap. In general, the level of the acoustic spectra with the 30° deflector fell between those for the two 40° deflector configurations.

Chordwise location of nozzle. - Moving the nozzles closer to the trailing edge (0.46 chord) generally increased the noise levels at the mid and high frequencies as shown in figure 23. The acoustic level of noise source I was not significantly affected by the nozzle relocation; however, the frequency at which the peak noise level occurred increased by one 1/3-octave band (from 400 to 500 Hz). Similar aero-acoustic trends were obtained with the 60° flap when the nozzle was relocated closer to the wing trailing edge. The increase in noise level at high frequencies reduced the amount of jet noise shielding when the nozzle was relocated closer to the wing trailing edge.

COMPARISON OF NOZZLE-WING CONFIGURATIONS WITH AND WITHOUT EXTERNAL DEFLECTOR

A comparison of the aero-acoustic characteristics of the reference 5:1 slot nozzle and the 40° full-lip external deflector with the 40/40 nozzle is made in figure 24 for the baseline wing.

For the 20° flap setting (fig. 24(a)), the acoustic spectra for the two configurations are quite similar; thus, the same amount of jet noise shielding is provided with both nozzle types. The external deflector configuration, however, is about 3 dB quieter in the region of the peak noise for noise source II than the cutback nozzle configuration. The aerodynamic characteristics of the two configurations are significantly different, with the cutback nozzle providing a much thicker (absolute value) jet shear layer at the wing trailing edge than that with the external deflector. Furthermore, the peak local velocity at the wing trailing edge with the cutback nozzle is nearly 60-percent higher than that with the external deflector. The difference in the peak noise level for source II between the two nozzle-wing configurations is believed due to these aerodynamic differences.

With the 60° flap setting (fig. 25(b)), the noise levels of source I for the two nozzles again are similar. However, noise source II is much quieter with the external deflector than that with the cutback nozzle (up

to 4 dB at the peak). At the higher frequencies, the cutback nozzle is slightly quieter than the external deflector (up to 1.5 dB at some frequencies), thus providing somewhat more jet noise shielding benefits. The increase in noise level for source II is again attributed to the greater jet shear layer thickness and higher velocities at the wing trailing edge for the cutback nozzle compared to those for the external deflector.

SHIELDING OF JET NOISE

Representative data of the shielding of jet noise by the wing is shown in figures 25 and 26 for the baseline wings. Also, included are data for a configuration using an external deflector, for which case the wing shields not only jet noise but also jet-deflector interaction noise. The data in figures 25 and 26 are shown in terms of ΔSPL (SPL of the specific nozzle-wing configuration minus the SPL of the reference 5:1 slot nozzle) as a function of frequency and were obtained from the spectral plots shown previously.

Effect of nozzle roof angle. - The ΔSPL increased with increasing roof angles (fig. 25) for nozzles with sidewall cutback. Although not shown, the ΔSPL for nozzles without sidewall cutback was nearly independent of nozzle roof angle. Furthermore, for these nozzles, the ΔSPL with the larger nozzle roof angles generally was less, depending on the nozzle-wing configuration, than that for the nozzles with sidewall cutback.

Comparison of data for the baseline wing with the 40/40 nozzle and with the reference 5:1 slot nozzle using the 40° full lip external deflector indicate that the ΔSPL is the same for the 20° wing flap configuration. However, for a 60° wing flap, the wing configuration with the cutback nozzle provided a somewhat greater ΔSPL (~2 dB) than that with the external deflector.

Effect of wing size. - The effect of wing size on ΔSPL is shown in figure 26 for the 40/40 nozzle. The ΔSPL, at a given frequency, increases with an increase in wing size. At the same time, the peak local velocity is decreased with an increase in wing size. The increase in ΔSPL appears to be related to both the wing size (shielding length) and the local velocity field at the wing trailing edge. The exact relationship remains to be established and is beyond the scope of this report.

Similar trends in the data to those shown in figures 25 and 26 were obtained with the other configurations tested and at the lower jet velocity of 200 m/sec.

CONCLUDING REMARKS

The results of this study have shown that the changes in the characteristics of the flow field at the wing trailing edge caused by changes in the geometry of the nozzle-wing configuration correspond to the acoustic

trends measured in the far-field. Decreasing the jet shear layer thickness and increasing the local Mach numbers at the wing trailing edge by means of nozzle geometry changes generally caused increases in the SPL values measured in the far-field. The use of aerodynamic parameters at the wing trailing edge including a jet shear layer thickness parameter, such as perhaps δ_e (ref. 6), the peak local Mach number, and as yet unidentified other critical local flow parameters appear to be needed in order to obtain a general correlation of the jet-surface interaction noise sources and the jet noise shielding benefits derivable from the wing.

Assessment of the nozzle geometry effects indicates that nozzle cutback is beneficial to both jet flow attachment to the flap surfaces as well as reducing the overall noise level. Maximum overall noise reduction benefits tend to be attained with an external deflector, which grossly represents a cutback nozzle with fully open sides. Optimization of the configuration for aero-acoustic performance appear achievable by properly adjusting the nozzle roof angle as well as the nozzle sidewall cutback. The acoustic differences between the cutback nozzles and those with an external deflector, however, are not great so that weight and mechanical features and/or cruise performance considerations may be the ultimate factor that determine the nozzle selection for a particular aircraft application.

A nozzle configuration which provides unattached flow for the cruise mode could prove to be a necessity for an operational configuration. Such a design could consist of a pylon-mounted engine nacelle at a sufficient height off the wing surface to minimize jet flow attachment during cruise. For the landing and takeoff modes, an external deflector would be used. In order to store the necessary external deflector, simplify design, and minimize weight, an inverted D-nozzle (flat side away from the wing surface) with an aspect ratio of about 2 could be a reasonable approach to an optimum configuration. Such an external deflector also could be made to serve as a thrust reverser for the landing mode.

Finally, scaling laws and flight effects for the present and other nozzle and deflector shapes and sizes must still be investigated before model scale data can be used with confidence to predict noise levels for full-sized aircraft.

NOMENCLATURE

(All symbols are in S.I. units unless noted.)

H	nozzle height
L	wing surface length downstream of nozzle exhaust plane
L_s	projected shielding length downstream of nozzle exhaust plane

M	Mach number
SPL	sound pressure level of nozzle-surface configuration, dB re $2/10^{-5}$ N/m^2
SPL_N	sound pressure level of nozzle only, db re $2x10^{-5}$ N/m^2
ΔSPL	$SPL-SPL_N$, dB
U	velocity
X,Y,x,y	wing surface contour dimensions (see fig. 4)
δ	jet boundary thickness characteristic dimension
θ	deflector lip angle
I,II	jet-surface interaction noise source identification

Subscripts

e	effective jet free shear boundary at wing trailing edge where the local Mach number is 0.8 M of peak local M
j	jet
m	maximum

REFERENCES

1. M. Reshotko, W. A. Olsen, and R. G. Dorsch, "Preliminary Noise Tests of the Engine-Over-the-Wing Concept. I. 30°-60° Flap Position," NASA TM X-68032 (1972).

2. M. Reshotko, W. A. Olsen, and R. G. Dorsch, "Preliminary Noise Tests of the Engine-Over-the-Wing Concept. 2: 10°-20° Flap Position," NASA TM X-68104 (1972).

3. U. von Glahn, M. Reshotko, and R. Dorsch, "Acoustic Results Obtained with Upper-Surface-Blowing Lift-Augmentation Systems," paper presented at 84th Meeting of the Acoust. Soc. Am. Miami Beach, Fla., Nov. 28-Dec. 1, 1972.

4. M. Reshotko, and R. Friedman, "Acoustic Investigation of the Engine-Over-the-Wing Concept Using a D-Shaped Nozzle," AIAA paper 73-1030 (1973).

5. M. Reshotko, G. H. Goodykoontz, and R. G. Dorsch, "Engine-Over-the-Wing Noise Research," AIAA paper 73-631 (1973).

6. U. von Glahn, and D. Groesbeck, "Acoustics of Attached and Partially Attached Flow for Simplified OTW Configurations with 5:1 Slot Nozzle," NASA TM X-71808 (1975) (Paper presented at 90th Meeting of the Acoust. Soc. Am., San Francisco, Calif., Nov. 1975) 1975.

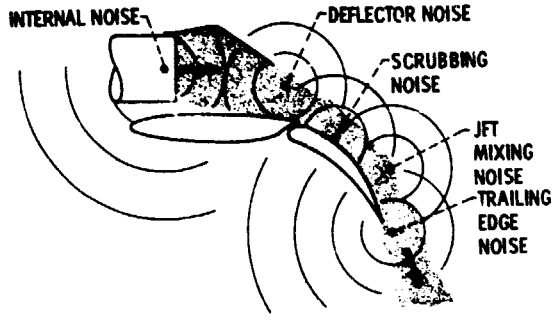

Figure 1. - Noise sources for engine-over-the-wing configurations.

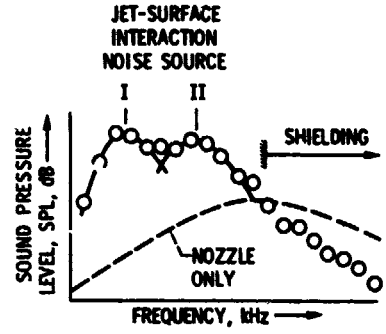

Figure 2. - Typical acoustic characteristics of an OTW configuration.

E-8519

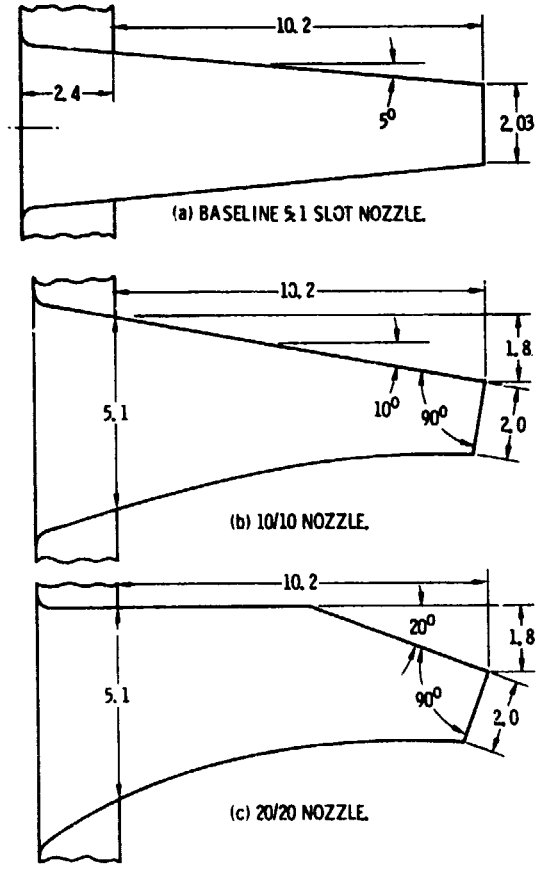

Figure 3. - Sketches of test nozzles and external deflectors. All nozzles were 10.2 cm wide. Dimensions in centimeters.

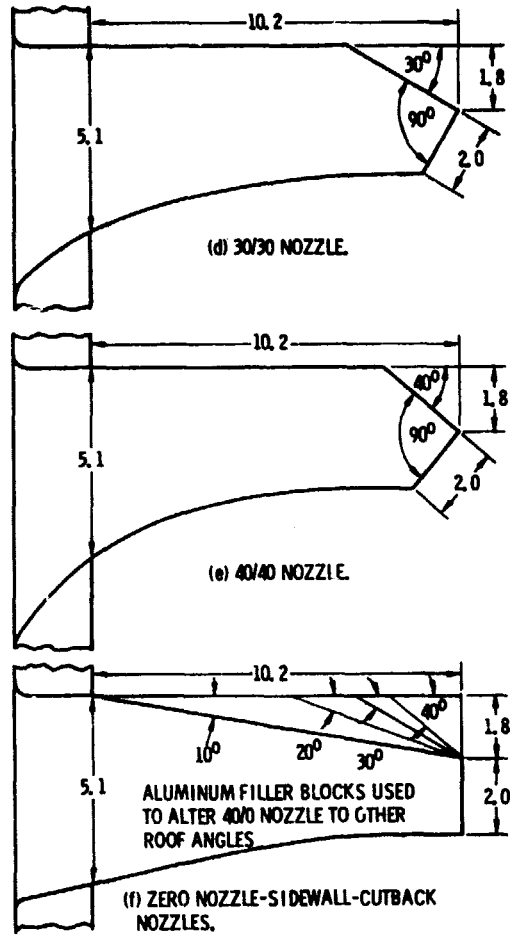

Figure 3. - Continued.

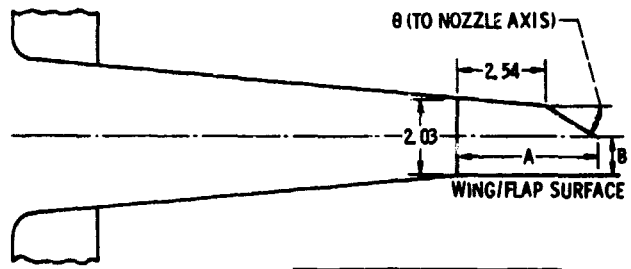

FLOP ANGLE, DEG	WING CONFIG-URATION	ℓ, CM	DEFLECTOR ANGLE, θ					
			30°		40°- FULL LIP		40°- ½ LIP	
			A	B	A	B	A	B
20	BASELINE	6.9	4.0	1.40	3.63	1.30	3.20	1.75
		15.2	↓	1.50	↓	1.40	↓	1.7[illegible]
60	BASELINE	6.9	↓	1.47	↓	1.40	↓	1.83
		15.2	↓	1.52	↓	1.42	↓	1.93

(g) DEFLECTOR DIMENSIONS (BASELINE 5:1 SLOT NOZZLE). ALL DEFLECTORS WERE 15.2 CM WIDE.

Figure 3. - Concluded.

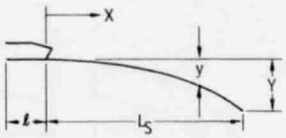

WING COORDINATES

FLAP ANGLE, DEG	WING CONFIGURATION	x/L_S / y/Y	0-0.4	0.5	0.6	0.7	0.8	0.9	0.95	0.975	1.0
20	2/3-BASELINE, BASELINE		0	0.04	0.13	0.26	0.44	0.70	0.85	-----	1.0
	3/2-BASELINE		0	0.25	0.10	0.225	0.42	0.7	0.85	-----	1.0
60	ALL		0	0.02	0.055	0.125	0.24	0.44	0.61	0.76	1.0

WING DIMENSIONS

FLAP ANGLE, DEG	CONFIGURATION	Y, CM	ℓ, CM	L_S, CM	L, CM
20	2/3-BASELINE	4.4 4.4	4.6 10.2	22.5 16.9	23.3 17.8
	BASELINE	6.6 6.6	6.9 15.2	33.8 25.4	35.4 27.0
	3/2-BASELINE	10.2 10.2	10.2 22.9	50.8 38.1	53.2 40.6
60	2/3-BASELINE	9.6	4.6 10.2	20.3 14.7	25.7 20.3
	BASELINE	14.3 14.3	6.9 15.2	30.5 22.1	38.7 30.2
	3/2-BASELINE	21.5 21.5	10.2 22.9	45.7 33.1	57.6 45.1

Figure 4. - Wing dimensions and coordinates. Dimensions in centimeters.

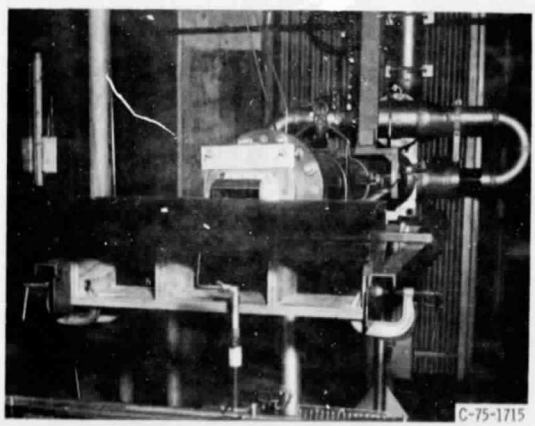

Figure 5. - Representative nozzle-wing configuration on test stand for flow field measurements.

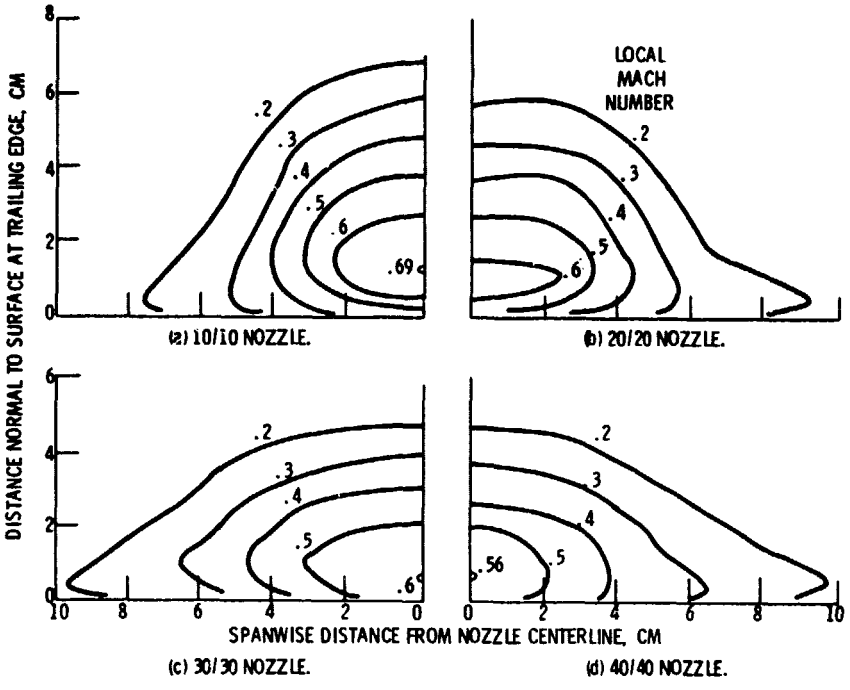

Figure 6. - Flow contour maps at trailing edge for baseline wing with cutback nozzles. 20^0 flap deflection; U_j, 266 m/sec; nozzles at 0.21 chord.

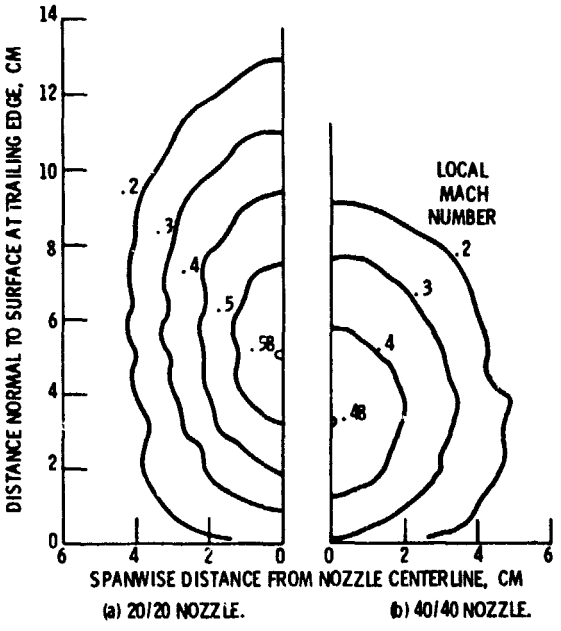

Figure 7. - Flow contour maps at trailing edge for baseline wing with cutback nozzles. 60^0 flap deflection; U_j, 266 m/sec; nozzles at 0.21 chord.

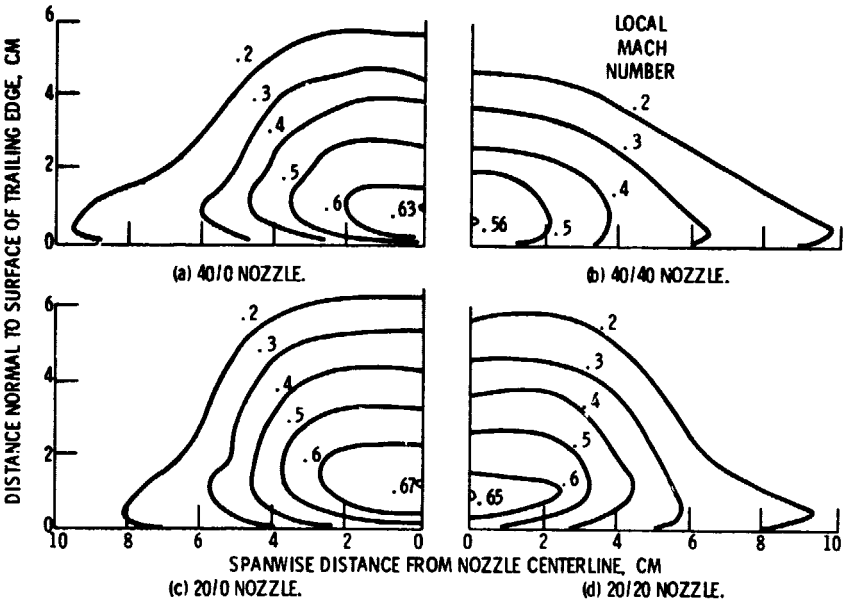

Figure 8. - Comparison of flow contours for baseline wing and nozzles with and without sidewall cutback. 20^{0} flap deflection; U_j, 266 m/sec; nozzles at 0.21 chord.

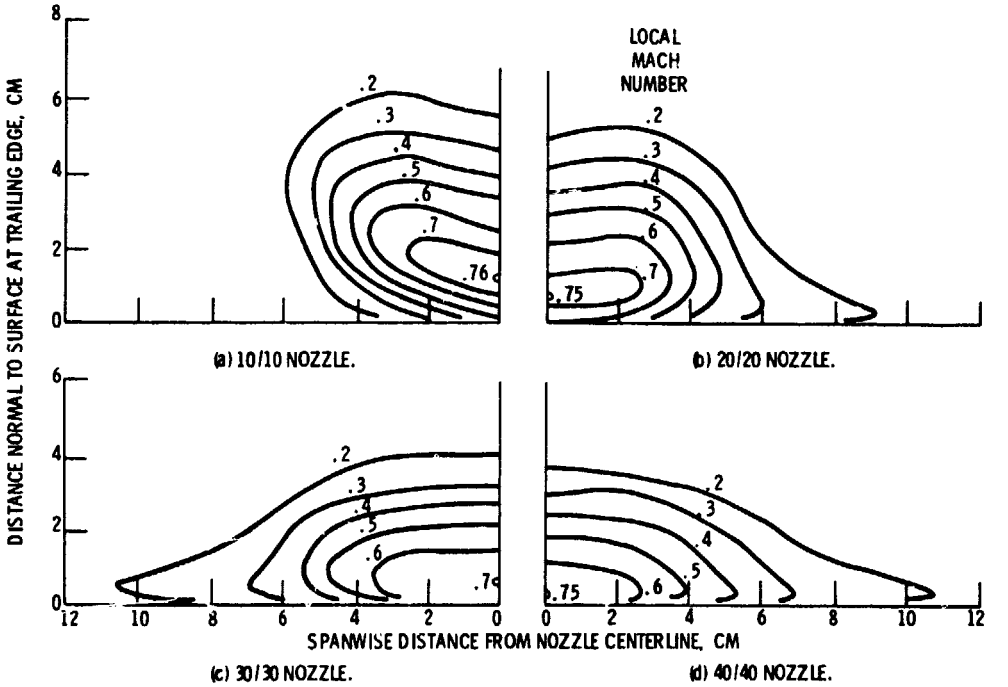

Figure 9. - Flow contour maps for baseline wing with cutback nozzles at 0.46 chord. 20^{0} flap deflection; U_j, 266 m/sec.

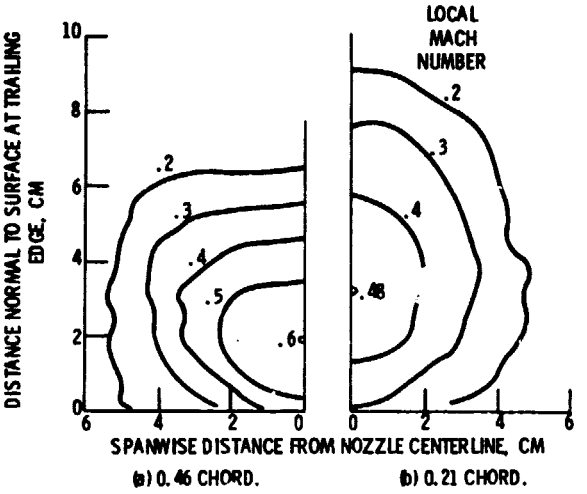

Figure 10. - Comparison of flow contours for baseline wing and 40/40 nozzle at two chordwise locations. 60° flap deflection; U_j, 266 m/sec.

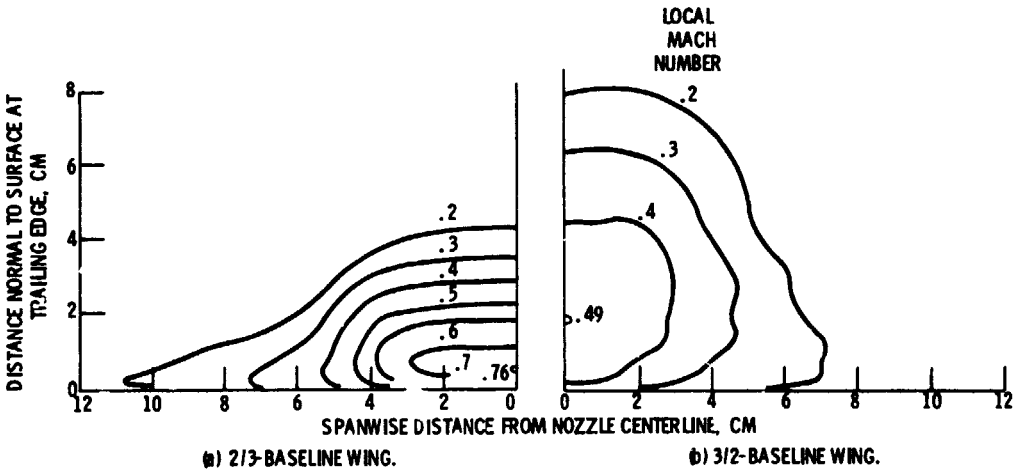

Figure 11. - Comparison of flow contours for two wing sizes using 20/20 nozzle. 20° flap deflection; U_j, 266 m/sec; nozzle at 0.21 chord.

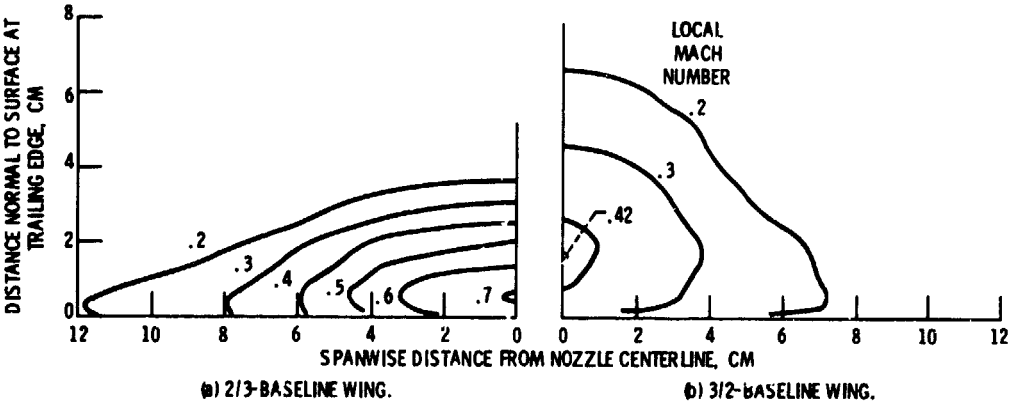

Figure 12. - Comparison of flow contours for two wing sizes using 40/40 nozzle. 20° flap deflection; U_j, 266 m/sec; nozzle at 0.21 chord.

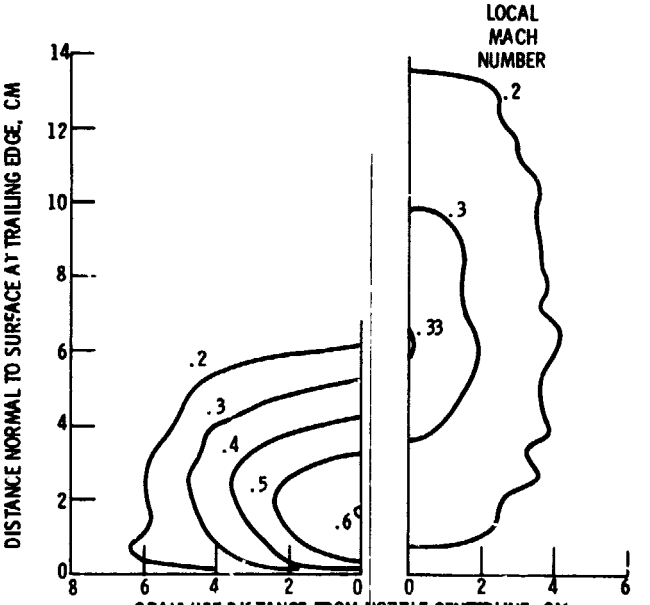

Figure 13. - Comparison of flow contours for two wing sizes using 40/40 nozzle. 60° flap deflection; U_j, 266 m/sec; nozzle at 0.21 chord.

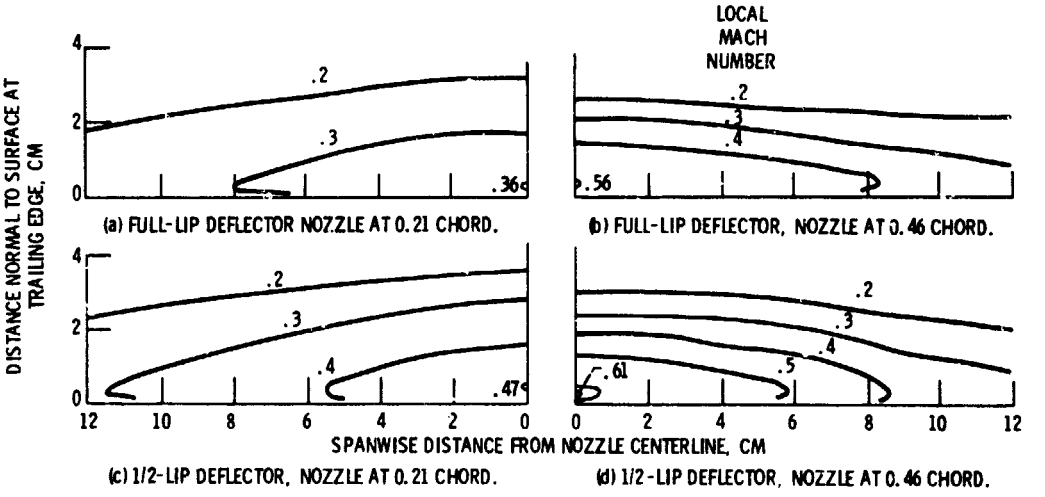

Figure 14. - Flow contour maps for baseline wing using reference 5:1 slot nozzle with 40° external deflector. 20° flap deflection; U_j, 266 m/sec.

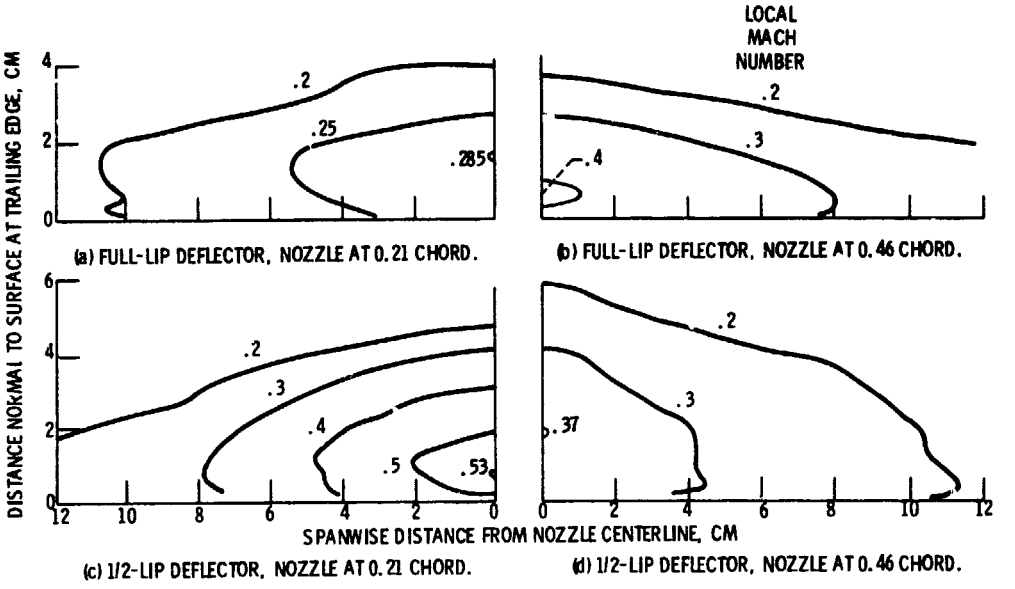

Figure 15. - Flow contour maps for baseline wing using reference 5:1 slot nozzle with 40° external deflector. 60° flap deflection; U_j, 266 m/sec.

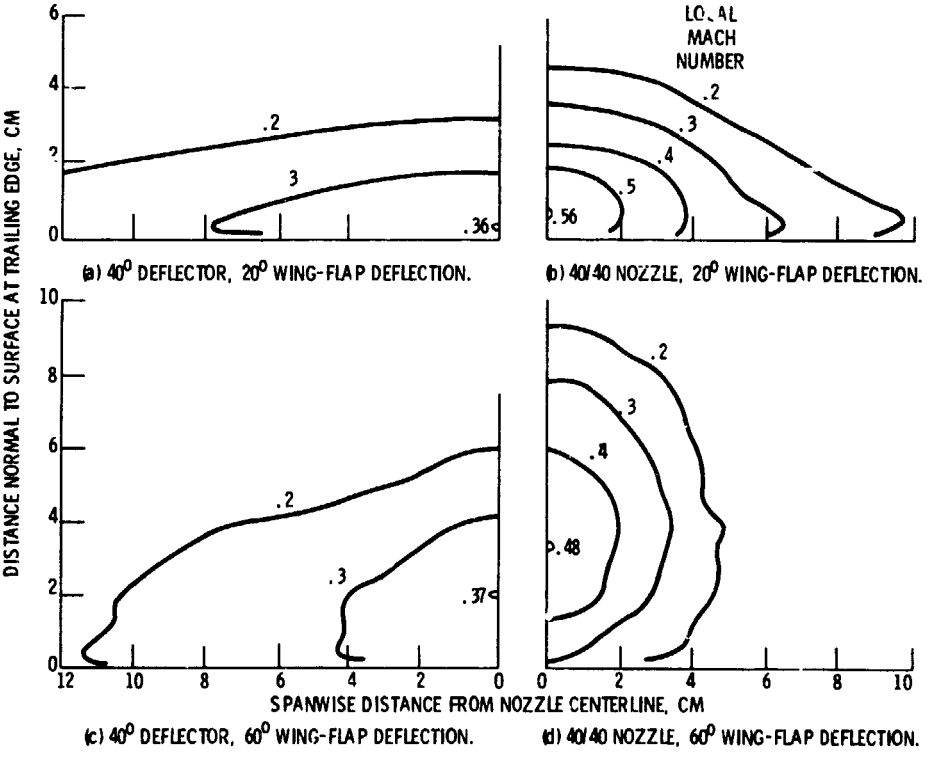

Figure 16. - Comparison of flow contours for baseline wings with 40/40 nozzle and with reference 5:1 slot nozzle using 40° full-lip deflector, U_j, 266 m/sec; nozzles at 0.21 chord.

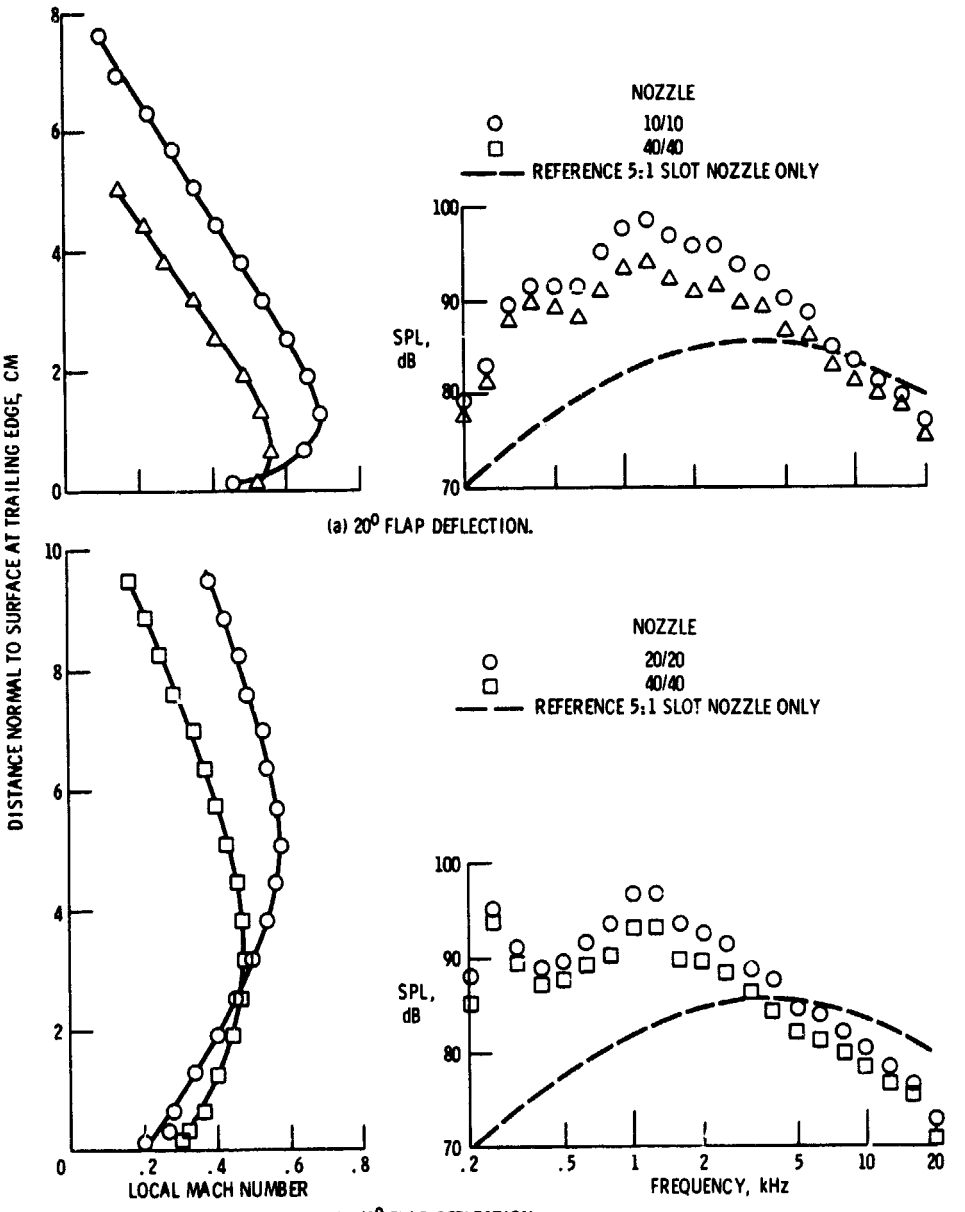

Figure 17. - Comparison of representative aero-acoustic characteristics for baseline wing with cutback nozzles. U_j, 266 m/sec; nozzles at 0.21 chord.

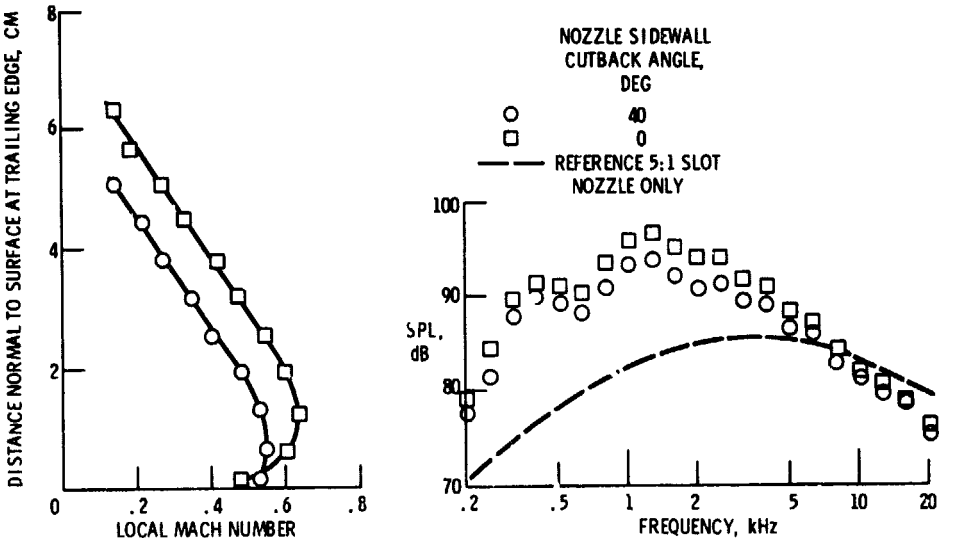

Figure 18. - Effect of nozzle sidewall cutback on aero-acoustic characteristics with baseline wing. Nozzle roof angle, 40°; U_j, 266 m/sec; nozzles at 0.21 chord; 20° flap deflection.

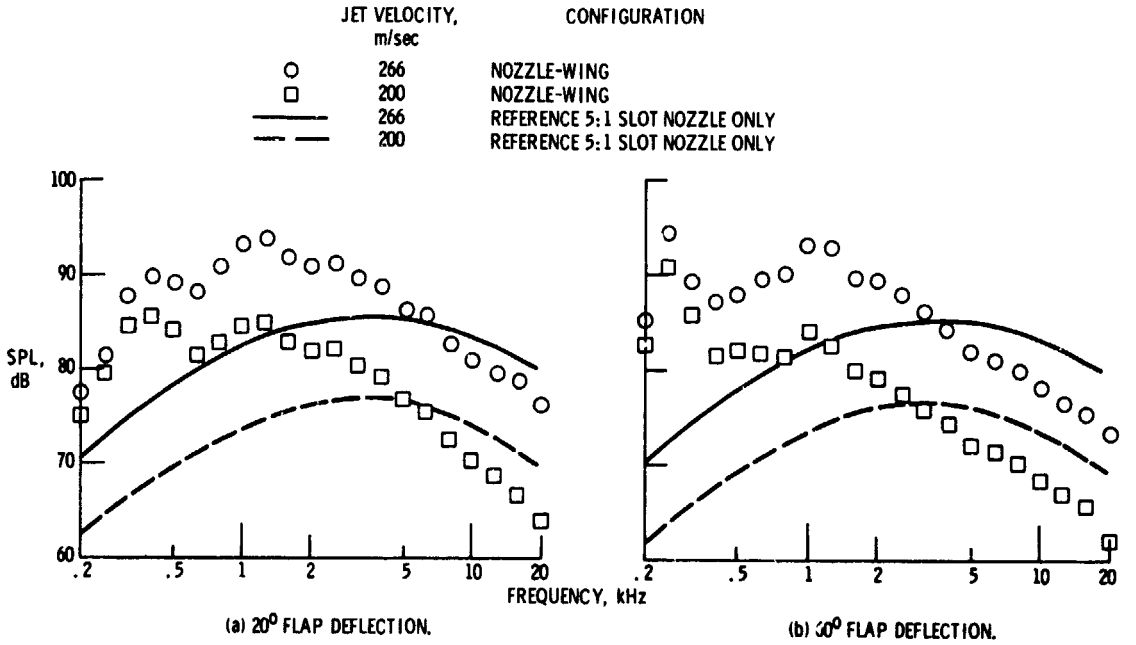

Figure 19. - Effect of jet exhaust velocity on spectra for baseline wings with 40/40 nozzle. Nozzle at 0.21 chord.

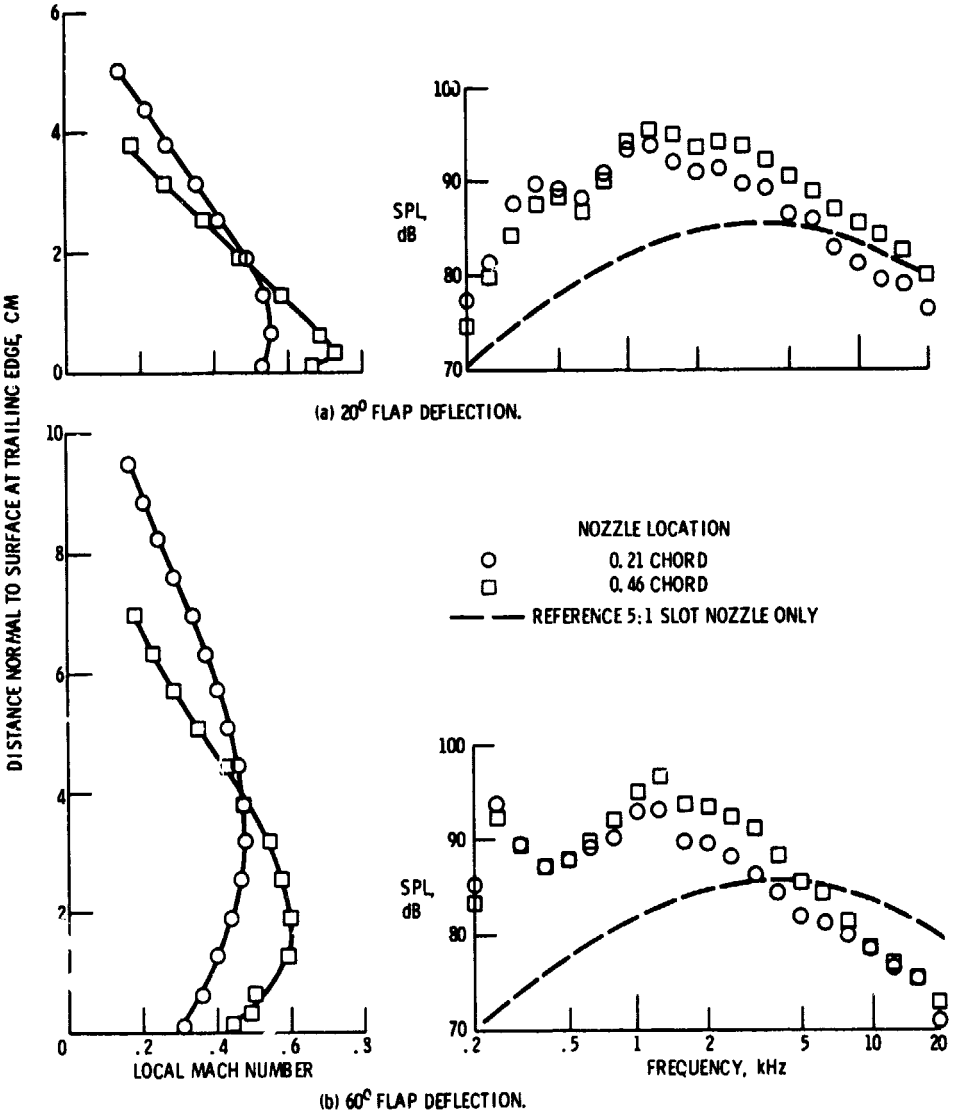

Figure 20. - Effect of nozzle chordwise location on aero-acoustic characteristics with baseline wings. 40/40 nozzle; U_j, 266 m/sec.

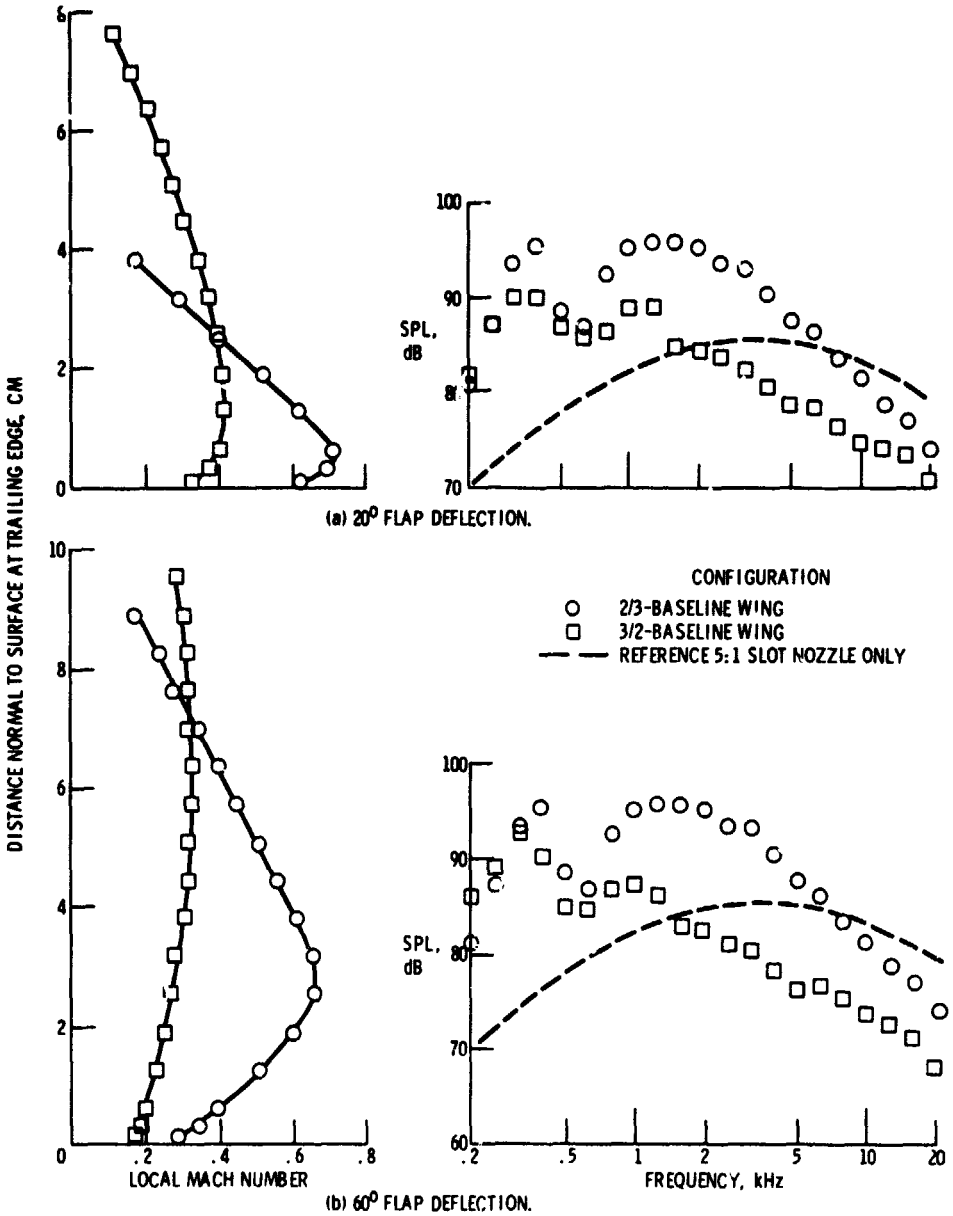

Figure 21. - Effect of wing size using 40/40 nozzle on aero-acoustic characteristics. U_j, 266 m/sec; nozzle at 0.21 chord.

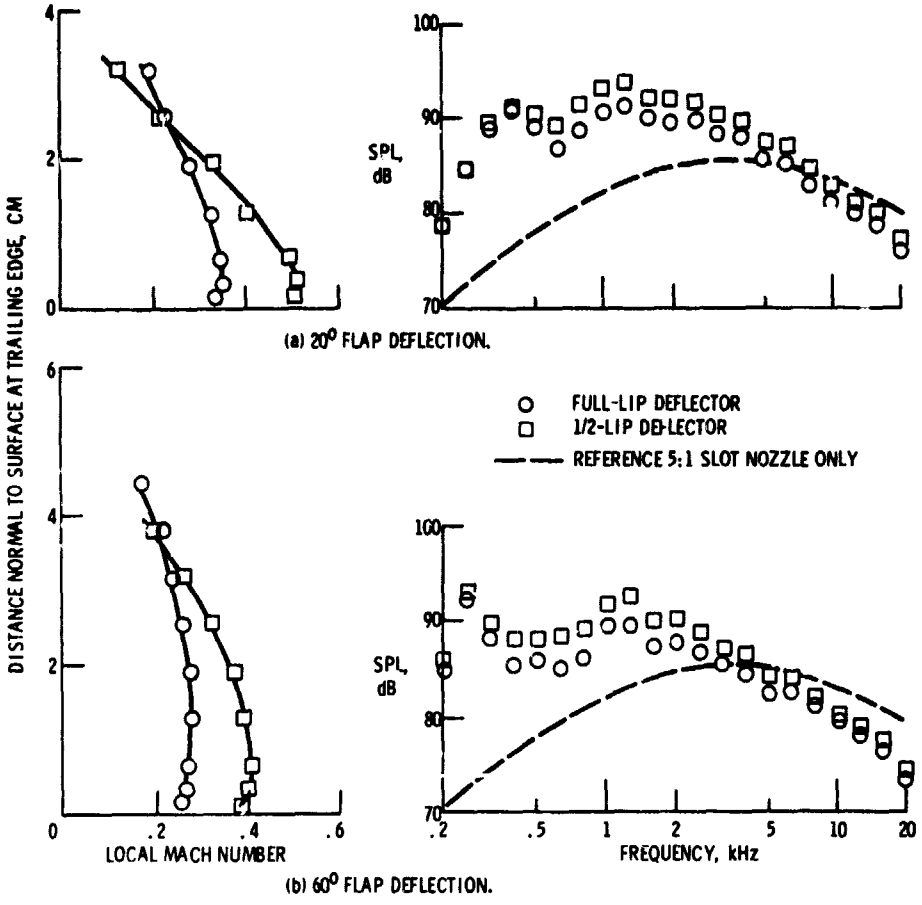

Figure 22. - Comparison of aero-acoustic characteristics for baseline wings with 40° full-lip and 1/2-lip external deflectors on reference 5:1 slot nozzle. U_j, 266 m/sec; nozzles at 0.21 chord.

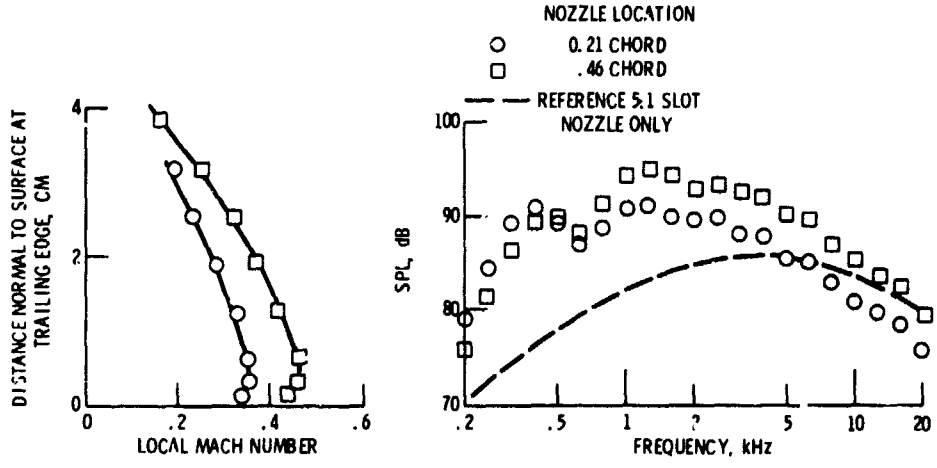

Figure 23. - Effect of nozzle chordwise location on aero-acoustic characteristics for baseline wing with reference 5:1 slot nozzle and 40° full-lip deflector. U_j, 266 m/sec; 20° flap deflection.

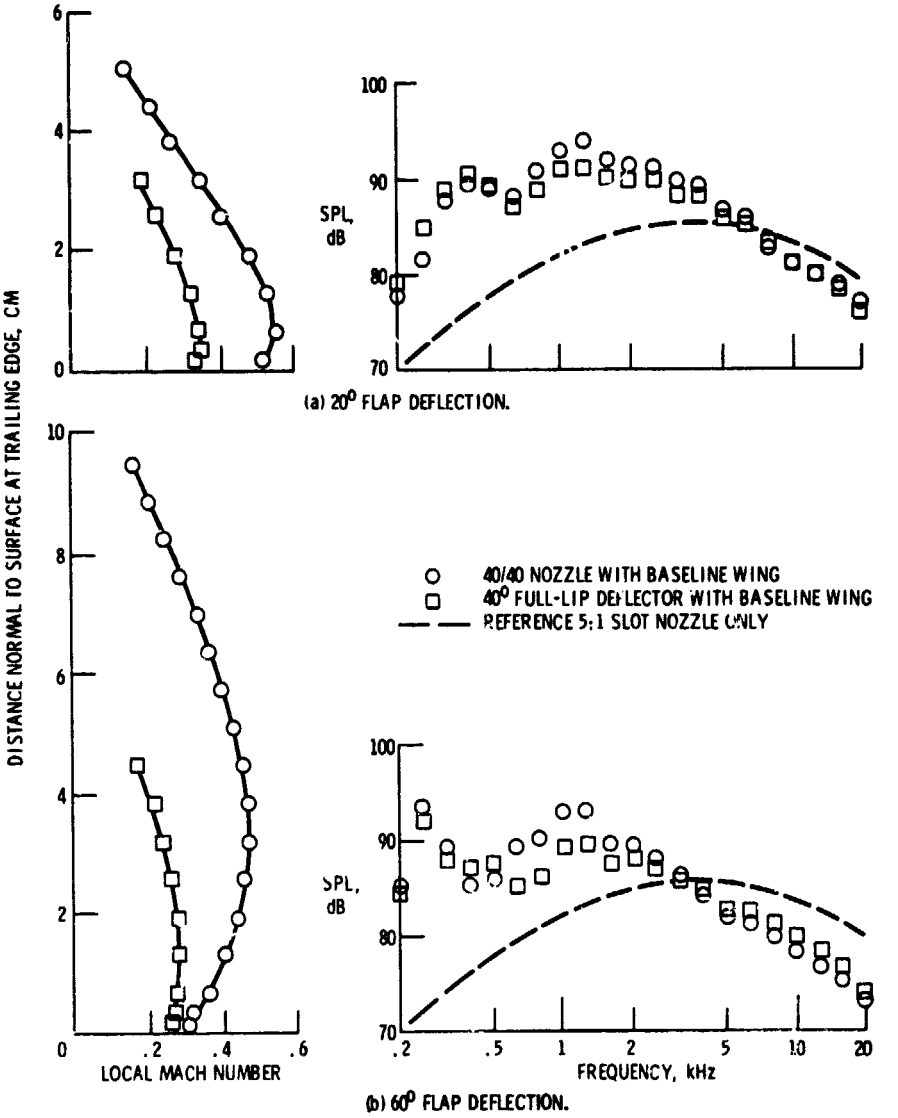

Figure 24. - Comparison of aero-acoustic characteristics for baseline wing with 40/40 nozzle and with reference 5:1 slot nozzle and 40° full-lip external deflector. U_j, 266 m/sec; nozzles at 0.21 chord.

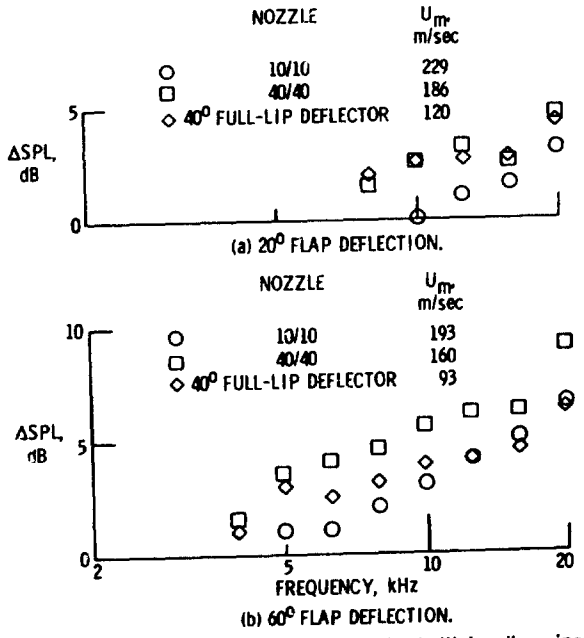

Figure 25. - Shielding benefits obtained with baseline wings and several nozzle configurations. U_j, 266 m/sec; nozzle at 0.21 chord.

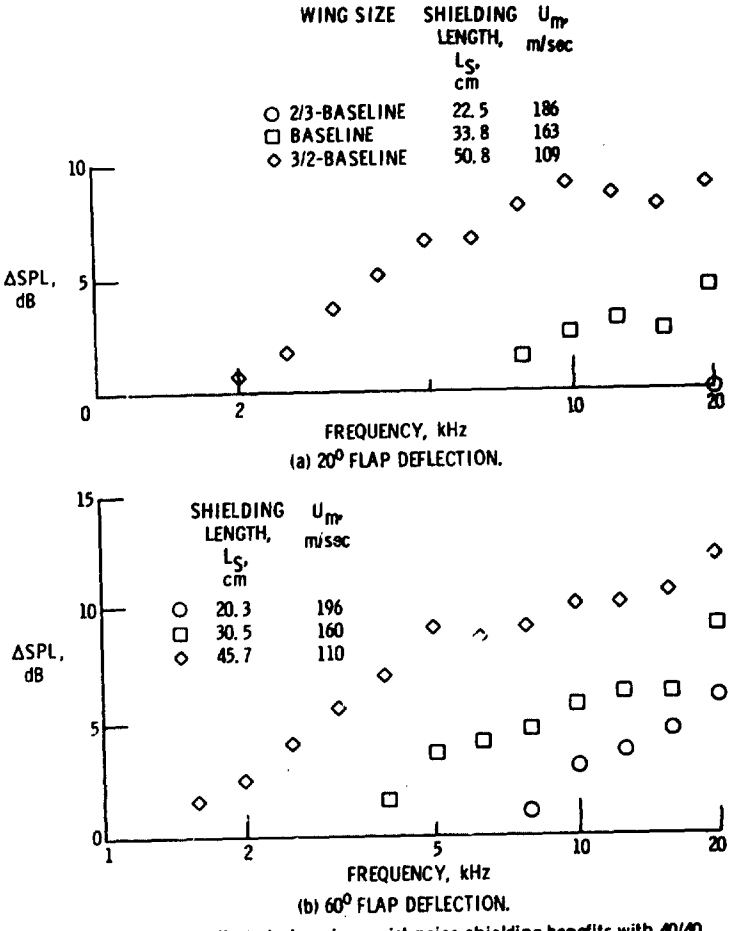

Figure 26. - Effect of wing size on jet noise shielding benefits with 40/40 nozzle. U_j, 266 m/sec; nozzle at 0.21 chord.